

Polymer Communication

Phase structure in polypropylene/PA6/SEBS blends

A.N. Wilkinson^{*}, L. Laugel, M.L. Clemens, V.M. Harding, M. Marin

Department of Chemistry and Materials, Manchester Metropolitan University, John Dalton Building, Manchester M1 5GD, UK

Received 29 October 1998; received in revised form 8 December 1998; accepted 8 December 1998

Abstract

A range of blends based on 70% by weight of polypropylene (PP) with 30% by weight dispersed phase were produced via melt blending in a co-rotating twin screw extruder. The dispersed phase composition was varied from pure Polyamide 6 (PA6) over a range of PA6 : SEBS (poly[styrene-*b*-(ethylene-co-butylene)-*b*-styrene]) ratios, using both reactive (maleic anhydride grafted) and non-reactive SEBS elastomers. The two-component PP/30%PA6 blend was unstable towards coalescence during melt processing and consequently exhibited a very coarse morphology and poor mechanical properties. Whereas a three-component PP/15%PA6/15%SEBS blend containing non-reactive SEBS exhibited two dispersed phases; a PA6 phase with a size-scale of 1–5 μm and an SEBS phase with a size-scale of $\leq 0.5 \mu\text{m}$. As a result both tensile and impact properties were much improved compared to the 70/30 blend. The use of reactive SEBS-*g*-MA resulted in the formation of dispersed phases consisting of PA6 particles encapsulated with SEBS. Varying the fraction of SEBS-*g*-MA in the dispersed phase allowed a manipulation of the dispersed phase structure, to form either core-shell PA6/SEBS particles or larger, more complex agglomerated PA6/SEBS structures. The core-shell particles resulted in an increase in Charpy impact strength of greater than an order of magnitude, compared to the PP matrix, and almost equivalent tensile properties. The larger agglomerated structures also generated very large increases in impact strength, of up to thirty-fold, but only at the expense of significant reductions in tensile modulus and yield stress. © 1999 Elsevier Science Ltd. All rights reserved.

Keywords: Multiphase polymer blends; Morphology; Phase structure

1. Introduction

The majority of commercial polymer blends possess a multiphase morphology, and satisfactory physical and mechanical properties in these materials are related to the presence of a finely dispersed phase which is resistant to gross phase segregation. Stabilisation of the blend morphology, or compatibilisation as it is usually termed, involves modification of the interfacial properties of the blend. Typically, this is achieved using block or graft copolymers with segments which exhibit intermolecular attraction and/or chemical reactions with the blend components; these copolymers concentrate at the interface between the blend components and act as emulsifiers, reducing interfacial tension and inhibiting coalescence during melt processing. Compatibilising copolymers are usually either formed *in situ*, by reactive compatibilisation [1] using suitably reactive monomers or polymers, or pre-formed and incorporated in a separate step. Reactive compatibilisation can also provide a degree of control over morphology development in multiphase polymer blends, via manipulation of the

interfacial energies within the system [2–7] which allows the formation of dispersed phases with a core-shell structure during a melt blending process [7–9]. This paper presents preliminary results of a study of PP-based blends with 30% by weight of a PA6/SEBS dispersed phase, using both reactive and non-reactive SEBS. Reaction between the PA6 and SEBS significantly reduces their interfacial energy, which acts both to encourage the SEBS to encapsulate the PA6 [6,7] and to stabilise the resultant multiphase morphology. In addition to the effects of interfacial reaction, this paper also presents results on the effects on morphology development of varying the ratio of PA6 : SEBS in the dispersed phase.

2. Experimental

The materials used in this study were: (i) an isotactic polypropylene homopolymer (PP), NovolenTM 1100H supplied by BASF (MFR 1.8 g 10 min, 230°C/2.16 kg), $T_m = 163^\circ\text{C}$); (ii) polyamide 6 (PA6), UltramidTM BS3 supplied by BASF ($M_n = 18\ 000 \text{ g mol}^{-1}$, $T_m = 220^\circ\text{C}$); (iii) poly[styrene-*b*-(ethylene-co-butylene)-*b*-styrene] (SEBS), KratonTM G1652 supplied by Shell Chemicals

^{*} Corresponding author.

E-mail address: a.wilkinson@mmu.ac.uk (A.N. Wilkinson)

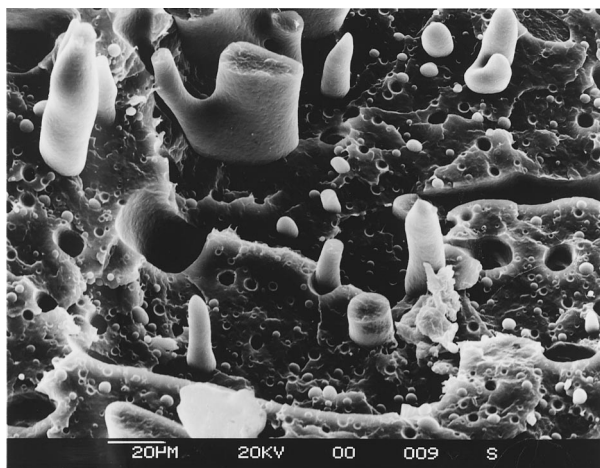


Fig. 1. SEM micrograph of the cryo-fractured surface of a 70/30 (PP/PA6) blend.

(30 : 70 styrene : EB), (iv) maleic-anhydride grafted poly[styrene-*b*-(ethylene-co-butylene)-*b*-styrene] (SEBS-*g*-MA), Kraton™ FG1901X supplied by Shell Chemicals (28 : 72 styrene : EB, 2% by weight maleic anhydride). Five blend compositions were studied, all with 30% by weight dispersed phase; a two-component blend, 70 : 30 PP : PA6, and four three-component blends, the first three consisting of PP/PA6/SEBS-*g*-MA: (i) 70 : 20 : 10, (ii) 70 : 15 : 15, (iii) 70 : 10 : 20 and the fourth of PP/PA6/SEBS:(iv) 70 : 15 : 15. The blends are designated using a number code referring to the weight ratio of the components (PP/PA6/SEBS) with reactive blends containing the grafted SEBS being identified by an additional letter (*g*). Prior to processing, the PA6 and the blends were vacuum-dried for at least 5 h at 80°C.

Melt blending was performed using a vented Betol BTS30 co-rotating twin-screw extruder (diameter of screws = 30 mm, length : diameter ratio = 21 : 1), the screw profile of which has been described in detail elsewhere [8]. Blend components were manually premixed then compounded using a screw speed of 70 rpm, an inverse temperature profile of 240°C (hopper) to 230°C (die) and a throughput of 8 kg/h⁻¹. The blends were extruded as twin laces of 4 mm diameter, which were hauled into a quenching water trough prior to being pelletised. Dried blends were moulded to form tensile and impact specimens using a Boy 15S injection moulding machine. The barrel temperature profile was 210°C (hopper) to 230°C (nozzle) and the mould temperature was maintained at 40°C.

Tensile stress–strain data were obtained at 25°C ± 2°C using a Hounsfield universal testing machine, according to BS2782. The strain in the sample up to 10% was recorded using a strain-gauge extensometer clamped directly to the neck of the specimen. Charpy impact strength was determined for notched specimens according to BS2782 using a Zwick 5102 pendulum-type instrument. Scanning electron microscopy was performed using a Cambridge Stereoscan

250 SEM. Samples for SEM were first cryo-fractured from liquid nitrogen. The resulting fracture surface was then either coated with gold/palladium alloy ready for imaging, or selectively etched to remove either the SEBS (using toluene) or the PA6 (using formic acid). Etching was performed at room temperature for 2 h, after which the surfaces were rinsed, dried, then coated with gold/palladium alloy. Transmission electron microscopy was performed using a Philips EM400 TEM at an accelerating voltage of 80–100 keV. Specimens of ~ 80 nm thick were prepared for TEM using a Reichert Ultracut ultramicrotome fitted with a diamond knife, then stained by exposure for 30 min to ruthenium tetroxide vapours generated from the oxidation of ruthenium dioxide by excess sodium periodate at ambient temperature [10].

3. Results and discussion

3.1. Microscopy

Fig. 1 shows an SEM micrograph of a cryo-fracture surface of the 70/30 blend. The dispersed phase of this uncompatibilised blend is unstable towards coalescence during melt processing and consequently forms a coarse morphology, consisting of both essentially spherical PA6 particles with size-scales of between 5 and 10 μm in diameter and larger, more complex domain structures. There is also evidence of poor interfacial bonding in this system, with particles of PA6 pulled from the PP matrix lying loose on the fracture surface. SEM of the three component blends revealed significant reductions in the size scales of the dispersed phases. Cryo-fracture surfaces of the 70/15/15 blend containing SEBS (Fig. 2(a)) revealed none of the complex morphology of the 70/30 blend, only a distribution of smaller PA6 particles, a reduction in size-scale which is to be expected upon reducing the weight fraction of PA6 from 30% to 15%. Etching of the fracture surface with formic acid revealed the presence of a broad distribution of predominantly spherical or slightly elongated (prolate) PA6 particles with diameters of between 1 and 5 μm (Fig. 2(b)). The specimens etched with toluene provided only poor quality images, but indicated the presence of a second, separate dispersed phase of predominantly spherical SEBS particles on a much smaller scale of between 0.1 and 0.2 μm. Specimens of the 70/15/15g blend etched with formic acid were also difficult to image, but indicated a further reduction in the size-scale of the PA dispersed phase to between 0.1 and 0.3 μm, as a result of the action of the reactive SEBS-*g*-MA. However, as it was not possible to clearly image the sub-micron dispersed phase morphologies of the three-component blends using SEM, TEM was subsequently employed.

TEM of RuO₄ stained specimens clearly revealed the morphologies of the three-component blends, as shown in Figs. 3 and 4 (a)–(c). The 70/15/15 blend containing SEBS

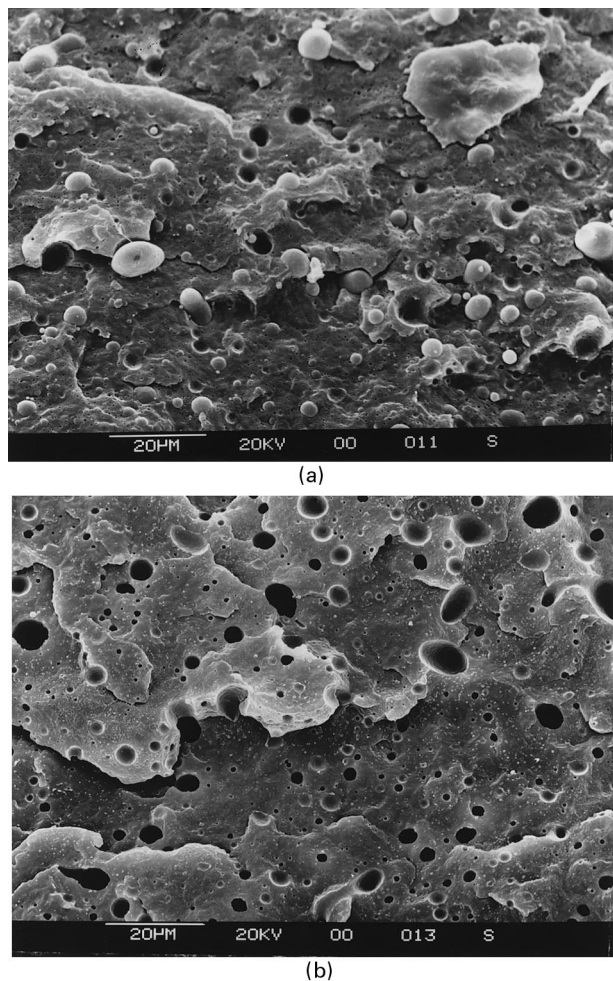


Fig. 2. SEM micrograph of (a) the cryo-fractured surface of a 70/15/15 (PP/PA6/SEBS) blend, and (b) the cryo-fractured surface after etching with formic acid to remove the PA6.

displayed a continuous–discontinuous type phase morphology. For example, Fig. 3 shows a large prolate spheroid-shaped PA6 particle, of approximately $4\ \mu\text{m}$ in length and $2\ \mu\text{m}$ in diameter, surrounded by a PP matrix containing predominantly spherical/prolate particles of SEBS (stained black by the action of the RuO_4) with dimensions $\leq 0.5\ \mu\text{m}$ and a relatively narrow size-scale distribution. In contrast, the three-component blends containing reactive SEBS-g-MA (Fig. 4(a)–(c)) displayed continuous–discontinuous morphologies in which a narrow size distribution of PA6 particles of $\leq 0.3\ \mu\text{m}$ were encapsulated by the SEBS, resulting from reaction between the maleic-anhydride grafts on the elastomer and the terminal amine groups of the PA6. All three blends in Fig. 4 contain 30% by weight (w/w) dispersed phase, but the ratio of PA6:SEBS-g-MA changes from 20 : 10 to 15 : 15 to 10 : 20 in Fig. 4(a)–(c). In the 70/20/10g blend (Fig. 4(a)), there are large numbers of individual prolate PA6 particles encapsulated to varying degrees by the SEBS (stained black by the action of the RuO_4) to form core-shell type structures. A degree of agglomeration of these particles is also visible (Fig. 4(a)), which increases

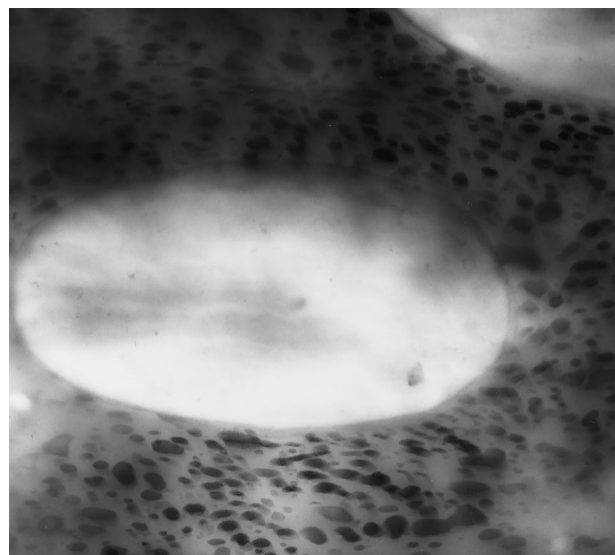


Fig. 3. TEM micrograph of the 70/15/15 blend containing SEBS, stained with RuO_4 (magnification $\times 30\ 000$).

significantly as the fraction of SEBS in the dispersed phase is raised (Fig. 4(b) and (c)). In comparison to Fig. 4(a), the dispersed phase morphologies displayed in Fig. 4(b) and (c) appear coarse, with large agglomerated structures containing PA6 particles encapsulated by SEBS, which are not dissimilar to the “salami” particle structures in rubber-toughened polystyrene.

3.2. Mechanical testing

The mechanical properties of the blends were compared to those of the matrix PP, which acted as a reference. The data from tensile and charpy impact testing are shown in Table 1. The 70/30 blend (containing 30% w/w of PA6) exhibited an increased tensile modulus and stress at break compared to the PP reference as a result of the reinforcing effect of the higher modulus ($\sim 2.75\ \text{GPa}$) higher yield stress ($\sim 70\ \text{MPa}$) PA6. However, the reinforcing effect of the PA6 dispersed phase is highly inefficient, owing to a combination of poor interfacial bonding between these immiscible polymers and the coarse dispersed phase morphology resulting from coalescence (Fig. 1). Thus, the 70/30 blend displayed significant reductions in yield stress and strain, strain at break and charpy impact strength compared to the PP reference. The 70/15/15 blend, in which the 30% w/w dispersed phase is split evenly between PA6 and SEBS, exhibited a much improved profile of mechanical properties compared to the 70/30 blend as a result of the significant change in morphology (Fig. 3); the SEBS dispersed phase acting to rubber-toughen the PP matrix whilst the well dispersed PA6 particles provided a degree of reinforcement. Thus, the 70/15/15 blend displayed only a statistically insignificant reduction in modulus compared to the PP reference and improved yield parameters compared to the 70/30 blend (but still much lower

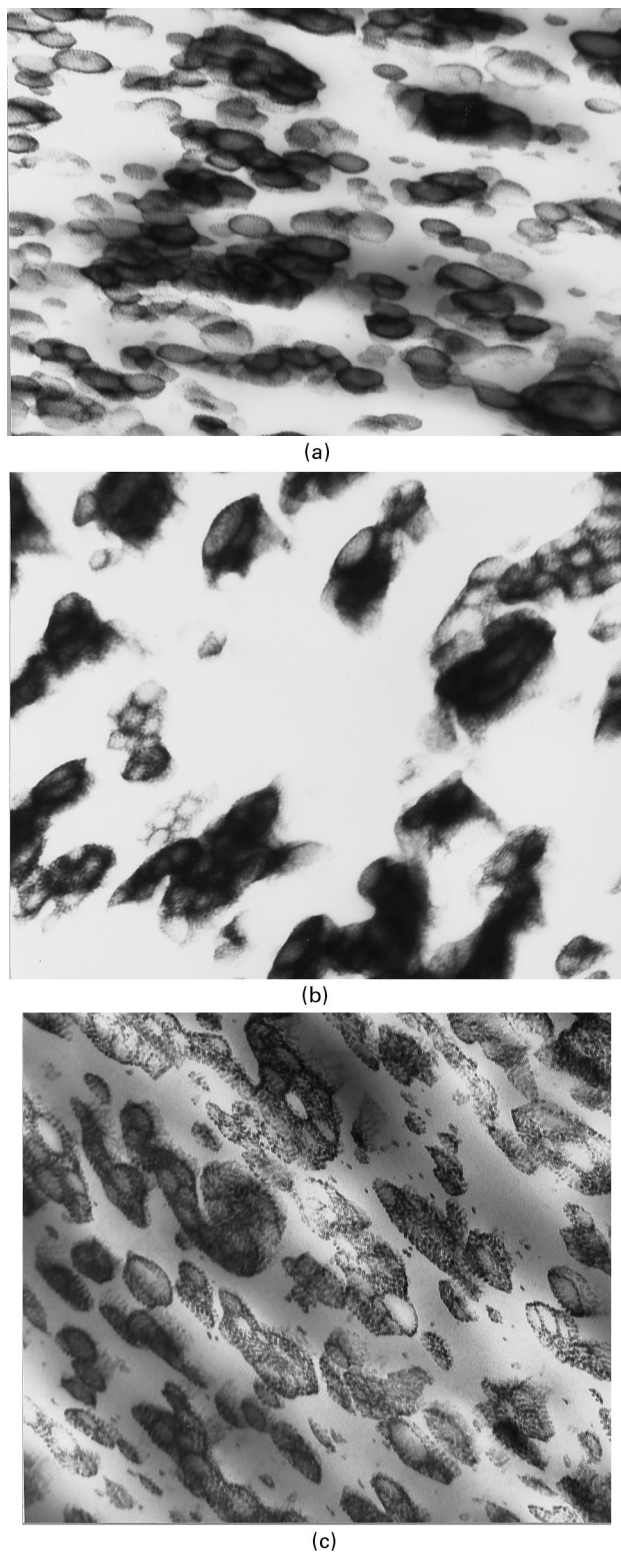


Fig. 4. TEM micrographs of blends containing SEBS-g-MA stained with RuO_4 (magnification $\times 65\,000$). (a) 70/20/10g, (b) 70/15/15g, (c) 70/10/20g.

Table 1
Mechanical properties of PP/PA6/SEBS blends (standard deviation in parentheses)

Material (PP/PA6/SEBS)	Secant modulus (MPa)	Yield stress (MPa)	Yield strain (%)	Stress at break (MPa)	Strain at break (%)	Charpy impact strength (kJ m^{-2})
PP (100/0/0)	1432 (47)	30.8 (0.7)	9.4 (0.3)	17.6 (0.7)	123 (12)	3.9 (0.4)
70/30/0	1636 (86)	22.3 (2.1)	3.7 (0.5)	21.1 (0.8)	5 (1)	1.3 (0.1)
70/15/15	1370 (93)	25.4 (0.3)	6.6 (0.2)	22.9 (1.1)	17 (2)	7.8 (0.8)
70/20/10g	1288 (31)	27.3 (0.8)	9.0 (0.8)	16.0 (1.1)	87 (16)	44 (5)
70/15/15g	951 (74)	22.8 (0.9)	12.3 (1.1)	16.5 (0.9)	163 (10)	52 (8)
70/10/20g	955 (59)	21.5 (0.4)	11.7 (0.9)	18.1 (1.0)	All > 400	107 (6)

than the PP reference), coupled with a significant increase in charpy impact strength. However, the greatest improvements in mechanical properties were exhibited by the blends containing SEBS-g-MA. The core-shell particles formed in the 70/20/10g blend (Fig. 4(a)) result in only relatively small drops in tensile parameters compared to the PP reference, but provide highly efficient toughening towards impact loading with an increase in charpy impact strength of over an order of magnitude. Increasing the fraction of SEBS-g-MA in the dispersed phase in the 70/15/15g and 70/10/20g blends resulted in significant reductions in modulus and yield stress compared to the PP reference with concomitant increases in ductility of the material. For example, the 70/10/20g blend exhibited approximate 30% reductions in modulus and yield stress in conjunction with a strain at break of $> 400\%$ (i.e. no break under test conditions) and an almost thirty-fold increase in charpy impact strength. Thus, the complex agglomerated PA6/SEBS-g-MA structures shown in Fig. 4(b) and (c) provide highly efficient toughening, but only at the expense of significant reductions in modulus and yield stress. It is interesting to note that the incorporation of SEBS-g-MA into the 70 : 15 : 15g blend results in a significantly lower modulus than that exhibited by the 70 : 15 : 15 blend containing non-reactive SEBS. If the 'rule of mixtures' relationship $E_{\text{blend}} = \sum \phi_i E_i$ is assumed to hold; the calculated modulus of the 70 : 15 : 15 blend is 1.46 GPa (assuming the modulus of the SEBS [11] to be 5 MPa), which is in reasonable agreement with the experimental value of 1.37 GPa, whereas the experimental modulus value of the reactive 70 : 15 : 15g blend is only 0.95 GPa. However, the latter value does agree well with the modulus calculated for a 70 : 0 : 30 blend (i.e. 70% PP : 30% SEBS) of 1.05 GPa. Thus in modulus terms, it appears that the agglomerated PA6/SEBS-g-MA phase of the 70 : 15 : 15g blend is acting more like pure SEBS-g-MA than a 50 : 50 mixture of PA6 and SEBS-g-MA, because of the encapsulation of the PA6 by the rubbery SEBS.

4. Conclusions

Blends based on 70% by weight of polypropylene with 30% by weight dispersed phase exhibited very different morphologies in electron microscopy and a wide range of mechanical behaviour. A two-component PP/30%PA6

blend was unstable towards coalescence during melt processing and consequently exhibited a very coarse morphology and poor mechanical properties. A three-component PP/15%PA6/15%SEBS blend exhibited two dispersed phases; a PA6 phase with a size-scale of 1–5 μm and an SEBS phase with a size-scale of $\leq 0.5 \mu\text{m}$. The resultant mechanical properties were much improved compared to the 70/30 blend, in particular charpy impact strength. The use of reactive SEBS-g-MA resulted in the formation of dispersed phases consisting of PA6 particles encapsulated with SEBS. Varying the fraction of SEBS-g-MA in the dispersed phase allowed a manipulation of the dispersed phase structure. Thus, either core-shell PA6/SEBS particles or larger, more complex agglomerated PA6/SEBS structures can be formed. The core-shell particles resulted in almost equivalent tensile properties to the PP reference, coupled with an increase in impact strength of greater than an order of magnitude. The larger agglomerated structures also generated very large increases in impact strength, of up to thirty-fold, but only at the expense of significant reductions in tensile modulus and yield stress.

Acknowledgements

We would like to thank Shell Chemicals and BASF for their kind donation of the materials used in this study, and Peter Carter and Sue Hutchinson for their help with TEM.

References

- [1] Xanthos M. Reactive Extrusion. Hanser, 1992.
- [2] Hobbs SY, Dekkers ME, Watkins VH. *Polymer* 1988;29:1598.
- [3] Cheng TW, Keskkula H, Paul DR. *Polymer* 1992;33:1607.
- [4] Guo HF, Packirisamy S, Gvozdic NV, Meier DJ. *Polymer* 1997;38:785.
- [5] Guo H-F, Gvozdic NV, Meier DJ. *Polymer* 1997;38:4915.
- [6] Rösch J, Mülhaupt R. *Makromol Chem Rapid Commun* 1993;14:503.
- [7] Rösch J, Mülhaupt R. *Polymer Bulletin* 1994;32:697.
- [8] Horiuchi S, Matchariyakul N, Yase K, Kitano T. *Macromolecules* 1997;30:3664.
- [9] Liauw CM, Lees GC, Hurst SJ, Rothern RN, Dobson DC. *Plast Rubb Comp Process Appln* 1995;24:249.
- [10] Trent JS. *Macromolecules* 1984;17:2930.
- [11] Holden G, Legge NR. Chapter 3. In: Legge N R, Holden G, Schroeder HE, editors. *Thermoplastic Elastomers*, Munich: Hanser, 1987.